Journal of Chromatography A, 1229 (2012) 148–155

Contents lists available at SciVerse ScienceDirect

Journal of Chromatography A

journal homepage: www.elsevier.com/locate/chroma

Gradient HPLC of samples extracted from the green microalga *Botryococcus braunii* using highly efficient columns packed with 2.6 μm Kinetex-C_{18} core–shell particles

Fabrice Gritti, Marie-Agnès Perdu, Georges Guiochon*

Department of Chemistry, University of Tennessee, Knoxville, TN 37996–1600, USA

ARTICLE INFO

Article history:
Received 13 November 2011
Received in revised form
19 December 2011
Accepted 2 January 2012
Available online 20 January 2012

Keywords:
Biofuels
Botryococcene hydrocarbons
Core–shell technology
Gradient elution
Peak capacity
Optimization

ABSTRACT

The analysis of the nonpolar extract of the cells of colonies of the green colonial microalgae *Botryococcus braunii* was performed by gradient HPLC. The growth of *B. braunii* was stressed by reducing its nitrogen nutrients by 90%, in order to enhance the production of nonpolar compounds. Highly efficient 4.6 mm × 100 mm columns packed with 2.6 μm Kinetex-C_{18} core–shell particles (Phenomenex, Torrance, CA, USA) were used. The gradient mobile phase was a mixture of acetonitrile and water (70–97%, v/v). Its initial and final compositions during the gradient elution were chosen so that the retention factors of the last eluted compound at the inlet and outlet of the column were 15 and 1, respectively. The highest peak capacity was obtained by optimizing several experimental parameters, including the injected sample volume, the flow rate, and the column length. The highest resolution was obtained by connecting one 4.6 mm × 150 mm and three 4.6 mm × 100 mm columns (total length 45 cm). The optimum flow rate was 1.5 mL/min, which provided the minimum plate height for the most retained compounds, the optimum inlet pressure was 930 bar and the injected volume 2 μL. The analysis time was then 14 min for a peak capacity of 121. The trends observed for the variation of the experimental peak capacity with the flow rate and the column length are in excellent agreement with theoretical predictions.

1. Introduction

The green colonial microalgae *Botryococcus braunii* is well known to produce large amounts of liquid hydrocarbon oils, which can be used as biofuels, are suitable to operate most ordinary diesel engines, and might provide a promising alternative to crude oils, when the world reserves of oils and gas will have been depleted and become scarce [1–4]. Three different races (A, B, and C) of *B. braunii* are recognized. Race B is much better documented. It produces C_{30}–C_{37} triterpenoid hydrocarbons with the general formula C_nH_{2n-10}, also called botryococcenes. Every such compound contains six double bonds. Today, up to fifty different botryococcenes have been identified using GC–MS spectrometry but only twenty such structures have been fully resolved [4]. Spectroscopic characterization of these hydrocarbons is limited, except by nuclear magnetic resonance [5] and Raman spectroscopy [6].

Before any structural characterization of a single botryococcene compound is attempted, several steps of separation, purification, and quantitation are necessary. Gas chromatography with flame ionization detector appears to be a suitable tool to achieve this task. Alkanes like *n*-C_{26} to *n*-C_{31}, squalane ($C_{30}H_{62}$), and squalene ($C_{30}H_{50}$, itself a botryococcene) are used as reference standard markers in order to measure the Kovats retention index and relative abundances of these hydrocarbons. Nevertheless, isolating about fifty different alkene compounds with molecular masses between 410 ($C_{30}H_{50}$) and 504 ($C_{37}H_{64}$) is a great challenge. Resolution rarely exceeds unity for closely eluted pairs of botryococcenes in GC because the elution window is relatively narrow. For instance, a typical GC run lasting about 45 min, with a 0.25 mm × 30 m capillary column, at a 1 mL/min flow rate of Helium carrier gas, and a linear temperature gradient from 60 to 300 °C, shows elution of botryococcenes during only the last 5 min [7]. Thus, a peak capacity of more than 100 should be achieved to fully resolve these complex mixtures. However, the highest peak capacity observed in such runs is only of the order of 70. Given that elution of these compounds follows a statistical distribution in time, they are randomly spread along the retention window, which explains why only two fifths of all possible botryococcenes have had their structures fully characterized up to now [4].

Surprisingly, liquid chromatography seems to never have been applied yet for the separation of botryococcenes. The recent progress made in column technology that took place over the last ten years [8,9] (with the commercialization of sub-2 μm fully

* Corresponding author. Fax: +1 865 974 2667.
E-mail addresses: guiochon@utk.edu, guiochon@ion.chem.utk.edu (G. Guiochon).

0021-9673/$ – see front matter © 2012 Elsevier B.V. All rights reserved.
doi:10.1016/j.chroma.2012.01.013

porous particles in 2004 and of sub-3 μm core–shell particles in 2006) and the development of two-dimensional liquid chromatography [10], now allow scientists to apply LC to rapidly separate highly complex samples. It should definitively be expected to resolve the fifty or so potential components of a botryococcene mixture by one-dimensional liquid chromatography. For instance, 4.6 mm I.D. columns packed with core–shell particles [11–14] may now provide up to 300 000 plates/m. One of the significant advantages of the columns packed with sub-3 μm core–shell particles over those packed with 2 μm fully porous particles is their larger permeability, which allows the achievement of similar resolution powers in a markedly smaller time. In gradient liquid chromatography, it was shown that a 10 cm long column packed with 2.6 μm core–shell particles could provide maximum peak capacities of 175, 100, and 50 for a protein digest mixture (β-Lactoglobulin) with ratios of the gradient time to the column hold-up time of about 15, 5, and 1, respectively [15].

In this work, a method was developed that allows a maximum peak capacity in excess of 100 to be reached in about 15 min for a complex mixture of the nonpolar compounds produced by *B. braunii*, by using a set of 4.6 × I.D. columns packed with 2.6 μm Kinetex-C_{18} particles. In order to reduce as much as possible both the analysis time and the solvent consumption, at the cost of certain loss in peak capacity, two constraints were self imposed: (1) the elution of the sample components should be spread over almost the whole gradient time, t_G and (2) the elution time of the last compound should be about one hold-up time less than the gradient time. Then, the injected sample volume, the flow rate, and the column length are optimized in order to maximize the peak capacity. All experimental peak capacities achieved are compared to those predicted by the gradient theory assuming either the absence [16] or the presence [17–22] of band compression during the gradient run.

2. Theory

2.1. Peak capacity

The theory of gradient elution chromatography is well established [23,24]. The underlying theory required to assess the quality of a separation in gradient elution was developed [16] based on the definition of the peak capacity, P_c, which is defined as the upper limit of the number of resolvable components assuming a resolution of unity or:

$$P_c = 1 + \int_{t_0}^{t_{last}} \frac{1}{4\sigma} dt \tag{1}$$

where t_0 is the column hold-up time, t_{last} is the retention time of the last eluted peak, t is a dummy time variable, and σ is the average time standard deviation of the peaks eluted during the gradient run between times t and $t + dt$. Note that Eq. (1) assumes that the dwell volume of the instrument is negligible.

During gradient elution, the rear part of the sample zone moves faster than its front part because the eluent strength increases constantly with passing time along the column. This phenomenon is better known under the name of band compression and can be theoretically calculated under certain conditions [17].

First, if we assume that band compression is negligible during the gradient run, the expression of the peak capacity is given by [16]:

$$P_c = 1 + \frac{1}{4}\sqrt{\frac{L}{H}}\frac{1}{G+1}\ln\left[\frac{G+1}{G}e^{Gk_F} - \frac{1}{G}\right] \tag{2}$$

where L is the column length, H the height equivalent to a theoretical plate under isocratic conditions (H is assumed constant at all mobile phase compositions), G is the intrinsic gradient factor, and k_F is the apparent retention factor of the last compound eluted during the gradient run. The gradient factor is written as:

$$G = S\Delta\varphi\frac{t_0}{t_G} \tag{3}$$

where S is the slope of the relationship between the natural logarithm of the retention factor, k, measured under isocratic conditions and the organic solvent concentration, φ, in the case when the linear solvent strength (LSS) model ($\ln k = \ln k_0 - S\varphi$) applies, $\Delta\varphi$ is the change in solvent composition during the gradient, and t_G is the gradient time. Note that Eq. (2) assumes that G is constant for all components in the mixture.

Finally, k_F for the last eluted compound is given by the parameters S and k_0 [16]:

$$k_F = \frac{1}{G}\ln[1 + Gk_{last}] \tag{4}$$

where k_{last} is the retention factor of this compound at the beginning of the gradient run.

Obviously, H is not necessarily constant over the range of mobile phase composition applied during the gradient. Therefore, the average value of the HETP, $\overline{H}$, experienced by the sample components during gradient elution should be used instead. It is given by [18]:

$$\overline{H} = \frac{t_G}{t_0}\frac{1}{\Delta\varphi}\int_{\varphi_{z=0}}^{\varphi_{z=L}}\frac{H(\varphi)}{k(\varphi)}d\varphi \tag{5}$$

where $\varphi_{z=0}$ and $\varphi_{z=L}$ are the mobile phase compositions eluting a given compound at the inlet and outlet of the column, respectively.

Secondly, if the band compression factor is taken into account in the expression of the peak capacity, we obtain [15]:

$$P_c = 1 + \frac{1}{4}\sqrt{\frac{3L}{\omega H}}\ln\left[\frac{2\omega e^{Gk_F} + G^2 - 6 + \psi}{G\left(2\sqrt{3\omega} + 3G + 6\right)}\right] \tag{6}$$

where

$$\omega = G^2 + 3G + 3 \tag{7}$$

$$\psi = 2\sqrt{\omega[(G^2-6)e^{Gk_F} + \omega e^{2Gk_F} + G^2 - 3G + 3]} \tag{8}$$

It is important to underline that in writing Eqs. (2) and (6) it was assumed that (1) the gradient profile is strictly linear and propagates at the same velocity as the chromatographic velocity, u_0; (2) H is constant, independently of the mobile composition; (3) G (or the LSSM parameter S) is the same for all the compounds eluted between $t = t_0$ to $t = (1 + k_F)t_0$; and (4) the dwell volume of the instrument is neglected.

3. Experimental

3.1. Chemicals

Acetonitrile, methanol, water, isopropanol, and chloroform were purchased from Fisher Scientific (Fair Lawn, NJ, USA). Acetonitrile, methanol, isopropanol, and water were of HPLC grade. Chloroform was of reagent grade. The mobile phase (acetonitrile/water) was filtered before use on a surfactant-free cellulose acetate filter membrane, 0.2 μm pore size (Suwannee, GA, USA). Squalene (>99% purity) and citric acid were also purchased from Fisher Scientific. The green microalgae *B. Braunii showa* (race B) was purchased from the University of Berkeley, CA, USA. The salts KNO_3, K_2HPO_4, $MgSO_4{\cdot}7H_2O$, $CaCl_2{\cdot}6H_2O$, ferric citrate, NaCl, and NaOH were all purchased from Fisher Scientific.

3.2. Apparatus

The 1290 Infinity HPLC system (Agilent Technologies, Waldbroen, Germany) liquid chromatograph used in this work includes a 1290 Infinity Binary Pump with Solvent Selection Valves and a programmable auto-sampler. The injection volume is drawn into one end of the 20 μL injection loop. The instrument is equipped with a two-compartment oven and a multi-diode array UV–VIS detection system. The system is controlled by the Chemstation software. The dwell volume (*e.g.* the system volume from the mixing point of the two mobile phases to the injection valve) is equal to 130 μL (100 μL mixer volume). The sample trajectory in the equipment involves the successive passage of its band through the series of:

- A 20 μL injection loop attached to the injection needle. The design of the injection system is such that the volume of sample drawn into the loop is the volume of sample injected into the column.
- A small volume needle seat capillary (115 μm I.D., 100 mm long), $\simeq$ 1.0 μL, located between the injection needle and the injection valve. The total volume of the grooves and connection ports in the valve is around 1.2 μL.
- Two 130 μm 25 cm long Viper capillary tubes offered by the manufacturer (Dionex, Germering, Germany) were placed before and after the column. Their total volume is 7.4 μL.
- A small volume detector cell, 0.8 μL, 10 mm path.

Short 130 μm I.D., 5 cm long Viper capillary tubes (volume < 0.7 μL) were used to connect the different 4.6 mm × 100 mm columns.

The extrapolation to a zero flow rate of the average extra-column volume of the equipment, fit with the Viper capillary tubes and measured for 1.0 μL injections of uracil tracers in the flow rate range between 0.05 and 2.0 mL/min is 11.4 μL. According to the dimensions just cited, we should have expected a volume of 0.5 (injection volume) +1.0 (needle seat capillary) +1.2 (injection valve) +7.4 (inlet and outlet capillaries) +0.4 (detector cell)=10.5 μL. Given the relatively large specifications (± 20%) for the inner diameter of the connecting capillary tubes, these two values are in good agreement. We measured an offset time of about 0.04 s between the moments when the zero time is recorded and when the sample leaves the injection needle. Note that the extra-column peak variance measured with the Viper connector rapidly increases from 2.9 μL^2 at 0.05 mL/min to 11.5 μL^2 at 0.6 mL/min and remains nearly constant at higher flow rates.

3.3. Columns

We used four 4.6 mm I.D. columns (lengths 10, 10, 10, and 15 cm) packed with 2.6 μm Kinetex-C_{18} core–shell particles, generously offered by Phenomenex (Torrance, CA, USA). Their total average porosities are $\epsilon_t = 0.52 - 0.53$ [25,26] and their average mesopore size is 100 Å (before C_{18} derivatization). Their modified silica-C_{18} surface were fully endcapped, according to a proprietary process.

3.4. B. Braunii growth and stress conditions

A modified Chu-13 medium was prepared to culture *B. Braunii showa*. This medium has the following composition (kg m^{-3}): KNO_3 (0.2), K_2HPO_4 (0.04), $MgSO_4 \cdot 7H_2O$ (0.1), $CaCl_2 \cdot 6H_2O$ (0.08), ferric citrate (0.01), citric acid (0.1). The pH of the medium was adjusted with a 5 M solution of NaOH to 7.5 before sterilization. Two types of medium were prepared: a normal Chu-13 (see above compositions) and a 10% N Chu-13 with only 0.02 kg m^{-3} KNO_3. These two media allow us to investigate the influence of the nutrients on the growth curve of the microalgae and on their accumulation of hydrocarbons.

Before each extraction, we measured the amount of chlorophyll A with a fluorescence reader (TD700 fluorometer Turner designs) by using a 450 nm wavelength excitation filter (bandwidth 50 nm) and a 685-nm emission filter (bandwidth 30 nm). This allows us to compare the amounts of compounds produced per mass unit of microalgae during each culture.

3.5. Extraction of the hydrocarbon compounds

After a colony of *B. Braunii showa* has grown during seven consecutive days, an extraction process was performed, according to the Folch method. First, the algae culture is centrifuged during 1 h and a half at 2000 rpm, to separate algae and medium. The supernatant is then removed and the accumulated algae cells are collected at the bottom. The cells were lysed in a mixture of chloroform and methanol (2/1, v/v), using a volume of this solvent mixture about 20 times that of the tissue sample (1 g of cells for 20 mL solvent). After dispersion, the whole mixture is stirred during 15–20 min in an orbital shaker at room temperature.

The homogenate is centrifuged to recover the liquid phase, which is washed with 0.2 volume of a 0.9% NaCl solution (4 mL for 20 mL homogenate). After vortexing during a minute, the mixture is centrifuged at low speed (2000 rpm) to separate the two phases. The upper (aqueous) phase was removed with a pipet and kept to analyze gangliosides or small organic polar molecules. The lower chloroform phase containing the hydrocarbons, hydrocarbons and other hydrocarbon or weakly polar compounds is evaporated under vacuum in a rotary evaporator. Finally, the extracted compounds are collected in a small volume (5 mL) of isopropanol.

3.6. Hydrocarbon separation

Gradient HPLC was used for the analysis of the hydrocarbons produced by *B. Braunii*. The initial and final compositions of the acetonitrile/water mobile phase (70/30 and 97/3, v/v) were set so that the retention factor of the last eluted hydrocarbon compound was around 15 at the beginning of the gradient run and around 1.5 when it exited the column. In contrast to what is usually observed in gas chromatography [7,4,27], this ensures that the less retained botryococcenes are eluted very soon after the hold-up time. Furthermore, to spread the elution times of the hydrocarbons over the whole gradient window (gradient time t_G), the elution time of the most retained (which seems to be also the most abundant) hydrocarbon compound was adjusted at be one hold-up time shorter than the gradient time (see Section 4 for the methodology applied). Then, the mobile phase composition is abruptly increased to 100% acetonitrile and the column is washed with four column volumes. Finally, the column is equilibrated with the initial mobile phase composition (70/30, v/v) during 5 column volumes. This elution procedure provides a wide useful retention window, hence important gains in analysis time and solvent consumption. This also maximizes the peak height, hence minimizes the detection limits.

Fig. 1 shows a typical gradient chromatogram recorded with the 4.6 mm × 150 mm Kinetex column. to analyze the hydrocarbon extract collected after a seven day growth of *B. braunii* submitted to a nutrient stress (10% nitrogen-based nutrients).

4. Results and discussion

4.1. Impact of nutritional stress on the production of hydrocarbons

First, we checked whether a colony of *B. braunii* incubated during seven consecutive days under nutrient stress (10% nitrogen, only) produces a measurable amount of hydrocarbons compared to that produced by the same amount of microalgae incubated under

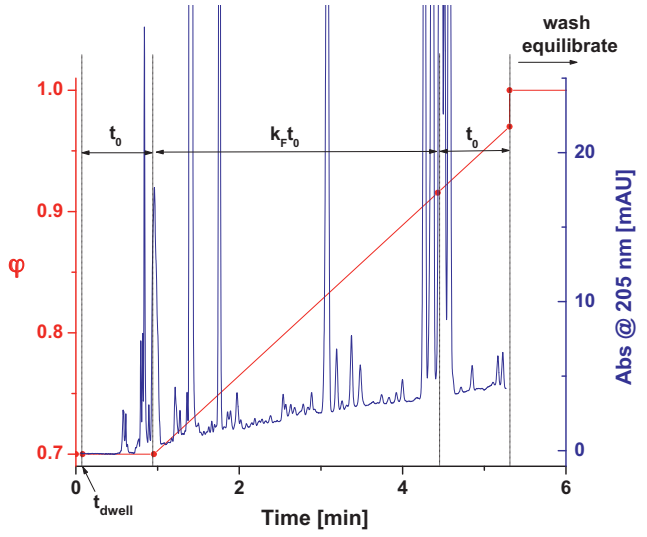

Fig. 1. Typical gradient elution run applied to minimize solvent and time consumption. The elution times of the most abundant botryococcenes are spread over the retention window of width $k_F t_0$. The last most abundant botryococcene is eluted at one hold-up time before the end of the linear gradient reaches the column outlet. The retention factors of the last eluted compound at the inlet and outlet of the column are $k_{z=0} = 15.0$ and $k_{z=L} = 1.6$, respectively. 4.6 mm × 150 mm 2.6 μm Kinetex-C_{18} column. $F_v = 1.50$ mL/min. $t_G = 4.7$ min. $t_0 = 0.87$ min. $t_{dwell} = 0.08$ min. $T = 297$ K.

normal nutrition conditions (100% nitrogen). Fig. 2 compares the chromatograms of the hydrocarbon samples extracted from these two cultures. The gradient conditions were not optimized for the sample corresponding to the stressed microalgae but the amplitude of the gradient was set to a larger value (from 20% to 97% acetonitrile) and the gradient time was longer (about 20 min) in order to capture and isolate a maximum number of analyte peaks.

Fig. 2 demonstrates that the concentrations of at least six compounds (see asterisks in the graph, elution times at 385, 565, 595, 730, 880, and 920 s) increase by more than 100% when the microalgae are stressed by a 90% depletion of the nitrogen content in their nutrient. Other chromatograms showed that squalene is eluted after the last eluted analytes, therefore, none of the components present in significant concentration in the extract solution

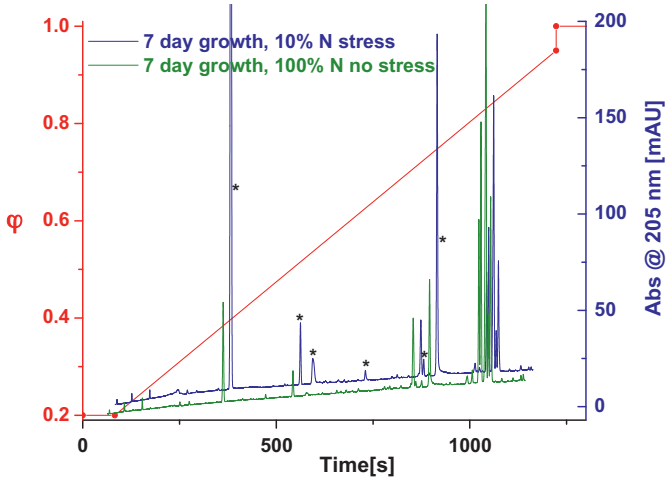

Fig. 2. Shift overlay showing the impact of the nutrition stress applied to *B. braunii* by depleting the nitrogen content in its nutrient by 90% for 7 consecutive days of incubation. The black asterisks flag the analytes the concentration of which increased by at least 100%. Conditions: 4.6 mm × 150 mm Kinetex-C_{18} column, mobile phase composition: 20–97% acetonitrile. $F_v = 1.50$ mL/min. $t_G = 19.0$ min. $t_0 = 0.85$ min. $t_{dwell} = 0.08$ min. $T = 297$ K.

is squalene. Most likely, the molecular masses of the hydrocarbons present in the extract are smaller than that of squalene (410 g/mol), probably around 300 for the most retained ones. For the sake of comparison, the retention times of these hydrocarbons are comparable to that of the polycyclic aromatic hydrocarbon naphtho[2,3-a]pyrene, which has a molecular weight of 302 g/mol. Therefore, one can expect that the hydrocarbons detected contain about 20–25 carbon atoms.

The gradient conditions used for the chromatogram in Fig. 2 were not optimized. This chromatogram contains wide time gaps with no detected peak; the first abundant analyte contained in these hydrocarbon extracts is only eluted after 385 s (the sum of the dwell and hold-up time is only 83 s). So, in the next Section 4.2, we set other arbitrary constraints in order to reduce both the analysis time and the volume of eluent consumed during the gradient run.

4.2. Measurements made under isocratic conditions

As previously described in the experimental Section 3.6, analytical constraints were set in order to minimize the analysis time and the eluent volume consumed. First, we imposed that the retention factor, k_{last}, of the most retained hydrocarbon produced by *B. braunii* (elution time of 1074 s in Fig. 2) to be around 15 at the beginning of the gradient. The mobile phase composition, φ_{start}, at the start of the gradient is then given by:

$$k_{last}(\varphi_{start}) = 15 \tag{9}$$

According to the retention indices measured in gas chromatography [7], the elution times of botryococcenes are typically spread between those of the normal alkanes n-C_{27} and n-C_{31} (Kovats indices between 2700 and 3100). In liquid chromatography, it is known that the logarithm of the methylene selectivity ($\log \alpha_{CH_2}$) on silica-C_{18} bonded phases eluted with a 70/30 (v/v) mixture of acetonitrile/water is close to 0.18 [28]. By analogy to gas chromatography, it is reasonable to anticipate that the retention factors of the less retained hydrocarbon compounds in the samples will be of the order of $15 \times 10^{-(31-27+1)\times 0.18} \simeq 2$ at the beginning of the gradient. We also decided to set the retention factor of the most retained hydrocarbon at 1 at the end of the gradient. So, the mobile phase composition, φ_{end}, at the end of the gradient is given by:

$$k_{last}(\varphi_{end}) = 1 \tag{10}$$

Then, we decided to impose that the gradient elution time of the most retained hydrocarbon be one hold-up time unit shorter than the time needed for the gradient end to reach the column outlet or $t_R = (t_0 + t_G) - t_0 = t_G$. So, the gradient time, t_G, should be given by the following relationship [16]:

$$t_R = t_G = t_0 + \frac{t_G}{S_{last}\Delta\varphi} \ln\left[1 + S_{last}\frac{\Delta\varphi}{t_G} k_{last}(\varphi_{start}) t_0\right] \tag{11}$$

where $k_{last}(\varphi_{start})$ is the actual retention factor of the last eluted hydrocarbon when it enters the column inlet and S_{last} is the best slope of the plot of the logarithm of the retention factor *versus* φ, assuming a linear solvent strength model (LSSM).

Due to these choices, the elution time of the less retained hydrocarbon in gradient elution has to be close to the hold-up time and that of the most retained hydrocarbon close to the end of the gradient time. As a consequence, both the analysis time and the eluent volume consumed during the run are lower than with other experimental conditions. As an illustration, Fig. 1 shows the time distribution of the eluted components when these new conditions are applied for the same flow rate as that used in Fig. 2 (F_v =1.5 mL/min).

In order to determine φ_{start} and φ_{end}, the variations of the retention factor of the last eluted hydrocarbon as a function of the mobile

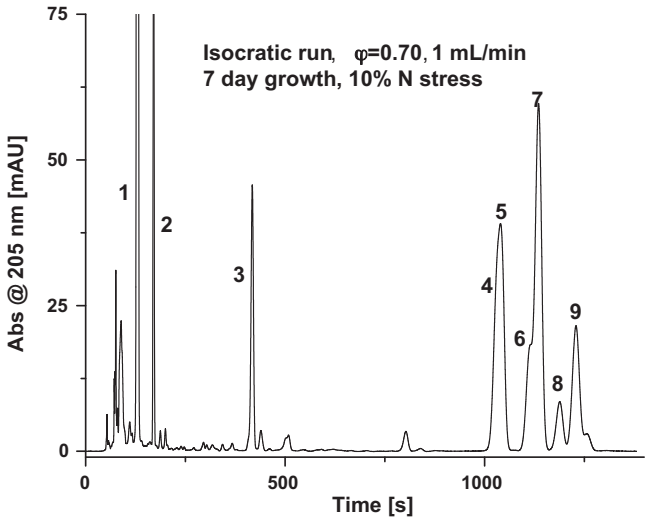

Fig. 3. Example of isocratic run of the hydrocarbon mixture. The nine most abundant analytes were detected as indicated in the graph. Acetonitrile/water eluent (70/30, v/v). F_v = 1 mL/min. T = 295 K. Note the long analysis time and the wide bandwidth of the last eluted hydrocarbon compound.

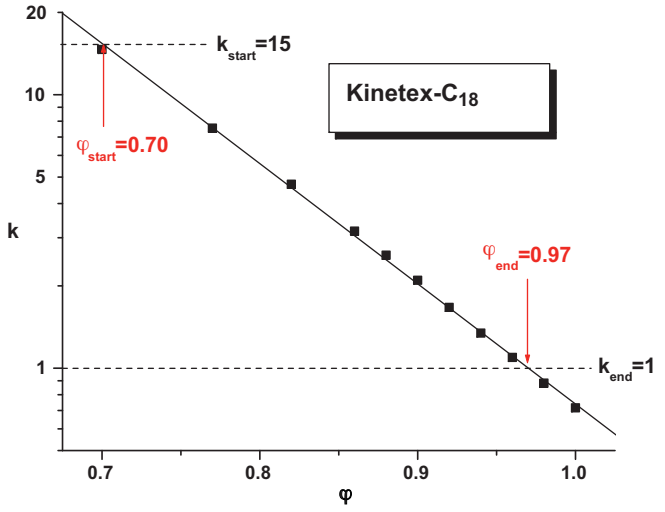

Fig. 5. Determination of the starting (φ_{start}) and ending (φ_{start}) acetonitrile concentration in the mobile phase given the constraints imposed to the retention factor of the last eluted compound at the beginning and the end of the linear gradient (k_{start} = 15 and k_{end} = 1).

phase composition, φ, were measured. Eleven 2 μL samples of the extract of the microalgae stressed for seven days were successively injected into a 4.6 mm × 150 mm Kinetex-C_{18} column and eluted with eleven mixtures of acetonitrile/water of decreasing concentrations, at a constant flow rate of 1 mL/min. The acetonitrile/water volume fractions (v/v) were 100/0, 98/2, 96/4, 94/6, 92/8, 90/10, 88/12, 86/14, 82/18, 77/23, and 70/30. The logarithm of the retention factors seems to follow well the LSSM, written as [21]:

$$\ln k = \ln k_0 - S\varphi \tag{12}$$

Fig. 3 shows the isocratic chromatogram of the hydrocarbon mixture for φ = 0.70. The retention factors of the nine most important peaks were measured for the chromatograms recorded with all the other mobile phases tested. Fig. 4 shows plots of the logarithm of the retention factors of these nine compounds *versus* the mobile phase composition, φ, confirming experimentally the validity of the LSSM for the retention behavior of these nine hydrocarbon compounds on the Kinetex-C_{18} adsorbent. We observed that the best slopes, S (obtained by adjusting the LSSM to the experimental plots of the retention factors ln k *versus* the acetonitrile composition φ), increase with increasing retention factors for the first four compounds, with S_1 = 5.60 to S_4 = 10.3. The S parameters of the last six compounds are close to each others, around 10.1 ± 0.2. Most likely, these six compounds have a similar number of carbon atom in their structure. Kinetex-C_{18} phases shows some interesting selectivity with respect to these six analytes but they cannot be fully resolved under isocratic conditions with φ = 0.70. Gradient elution is definitely necessary to achieve this goal. Knowing the accurate values of S_{last} and ln k_0 in Eq. (12), we can unambiguously determine φ_{start} = 0.70 and φ_{end} = 0.97 as shown in Fig. 5.

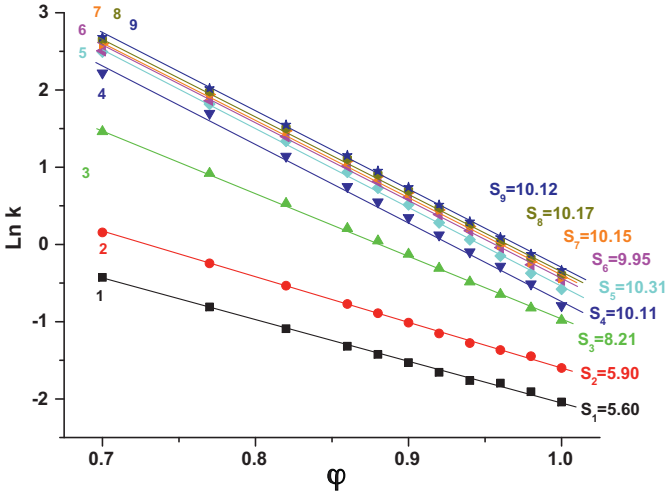

Fig. 4. Plot of the logarithm of the retention factors of the nine most abundant analytes *versus* the mobile phase composition in acetonitrile, φ.

4.3. Optimizing the gradient conditions

Finally, we need to optimize the gradient separation by selecting the most appropriate flow rate, injection volume, and column length.

4.3.1. Optimum flow rate

In this section, the column length was fixed at L = 15 cm. According to Eq. (11), when the flow rate F_v is selected (or $t_0 = \frac{V_0}{F_v}$), the gradient time, t_G, is also determined because φ_{start} (=0.70), φ_{end} (=0.97), S_{last} (=10.12), and $k_{last}(\varphi_{start})$ (=15) have already been imposed. The solution of Eq. (11) provides the unique experimental value of t_G/t_0 = 4.95, hence a unique value of G for all flow rates tested. The compromise set in this work from the constraints Eqs. (9)–(11) between a large peak capacity and a short analysis time provides a constant gradient factor G = 0.55 and an apparent retention factor for the last eluted compound k_F = 3.95. The injection volume was set at 2 μL. Ten flow rates were applied sequentially: 0.25, 0.50, 0.75, 1.00, 1.50, 2.00, 2.50, 3.00, 3.50, and 4.00 mL/min. The values of t_G were 25.9, 13.0, 8.6, 6.5, 4.3, 3.2, 2.6, 2.2, 1.9, and 1.6 min, respectively. Fig. 6 plots the experimental peak capacity as a function of the flow rate applied. Note that for the measurement of P_c, the experimental retention window starts at $t = t_0$ (hold-up time) and ends at $t = t_{last}$ (retention time of the last eluted compound) and the average peak width is computed from the average peak width measured for the last five compounds which have strictly the same S parameter of 10.1. The experimental peak capacity is then given by:

$$P_C = 1 + \frac{t_{last} - t_0}{(1/5)\sum_{i=1}^{i=5} w_i} \tag{13}$$

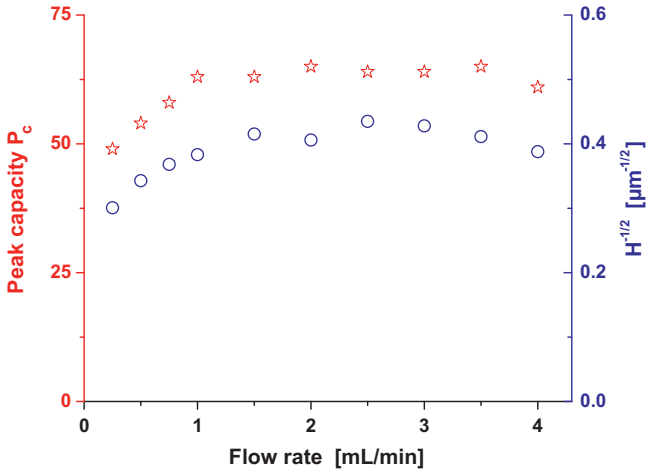

Fig. 6. Plots of the peak capacities and the reciprocal of the square root of the HETP measured for $\varphi = 0.70$ as a function of the imposed flow rate. Note the parallelism between the two plots.

The variations of these experimental peak capacities were compared to those predicted by the theory of gradient elution (Eqs. (2) and (6)). In Fig. 6, the plots of the experimental peak capacities, P_c, and of the reciprocal of the square root of the HETP, $1/\sqrt{H}$, as a function of the flow rate are shown for a mobile phase composition $\varphi = 0.70$. The plate heights, H, were computed from the average values measured for the last five compounds. It is noteworthy that the trends of both P_c and $1/\sqrt{H}$ are nearly parallel, in excellent agreement with the previsions of Eqs. (2) and (6). At all flow rates, the values of G and k_F remain constant (at 0.55 and 3.95, respectively). As the flow rate changes, the column HETP may change also and the variations of the peak capacity are directly related to the column HETP. Clearly, analysts should not operate at too low a flow rate, where the plate height is controlled by longitudinal diffusion. For the Kinetex column and the five last eluted hydrocarbons, this critical flow rate for which the HETP reaches its minimum is about 1.5 mL/min. On the other hand, the flow rate should not be too large because then the HETP increases due to heat friction.

The experimental and theoretical peak capacities were also compared at a flow rate of 1 mL/min. To predict the peak capacity in gradient elution, the reference average HETP experienced by analyte molecules during their elution has to be measured. Fig. 7 shows how the average HETP of the last five eluted compounds varies with increasing acetonitrile content in water from 70% to 98% (v/v). Remarkably, it is nearly constant around $H = 7$ μm for $\varphi < 0.90$, *e.g.* when the retention factors of these compounds exceed 2. For acetonitrile concentrations larger than 90%, the HETP steadily increases, up to about 13 μm, most likely because the trans-column velocity biases cannot be efficiently relaxed when surface diffusion and the residence times in the column decrease. The last compound elutes at $t = 414$ s. The acetonitrile composition at that time and at the column outlet (assuming piston flow displacement) is 0.7 +(0.27/392)×(414-79-7.5)= 0.93. The average HETP, $\overline{H}$, calculated according to Eq. (5) is then equal to 8.2 μm.

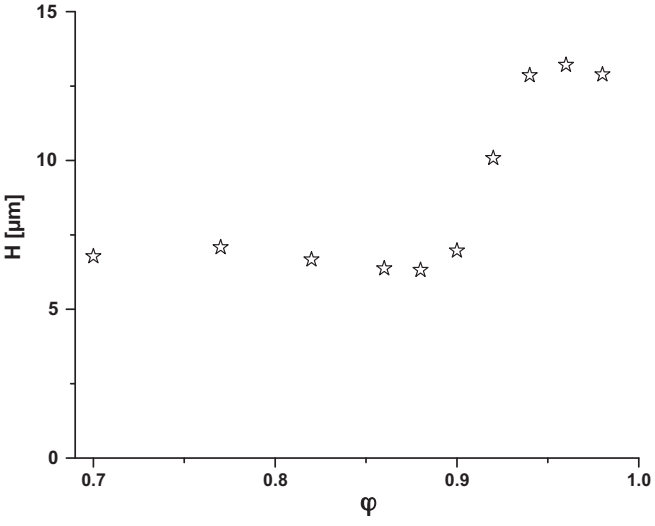

Fig. 7. Variation of the average column HETP of the five last eluted compounds with the acetonitrile content in the mobile phase, φ.

The predicted peak capacities are equal to 69 (assuming no band compression) and 79 when band compression is taken into account. The measured value was only $P_c = 63$. Therefore, the theoretical values of the peak capacity are incorrect because the assumptions made in the models used are certainly too simplistic. Both expressions of the peak capacity assume that (1) the gradient profile of acetonitrile is strictly linear and propagates at a linear velocity equal to the chromatographic linear velocity, u_0; (2) the HETP is constant in the range of mobile phase compositions experienced by the analytes during the gradient run; and (3) the dwell volume of the instrument is negligible.

The dwell time of the 1290 Infinity system at 1 mL/min is only 0.125 min whereas the column hold-up time and the gradient time are more than ten and fifty times larger at 1.31 min and 6.48 min, respectively. The dwell time can then be neglected in the calculations. The acetonitrile concentration varies from 0.70 to 0.93 during the elution of the last eluted compound, a range in which the column HETPs remain quasi-constant, at around 7–8 μm (see Fig. 7). The second and third hypotheses were thus valid in the gradient experiments conducted in this work. Therefore, if the theoretical models fail, it can only be due to the fact that the first hypothesis does not strictly apply. It is then important to check, in the present gradient conditions ($0.70 < \varphi < 0.97$), if the migration velocities of the acetonitrile concentrations remain constant and equal to the chromatographic linear velocity, u_0, for endcapped silica-C_{18} stationary phases.

A wealth of literature has been devoted to the measurement of the excess adsorption isotherms of organic solvents (methanol, acetonitrile, THF, *etc.*) aiming at characterizing chromatographic sorbents and investigating adsorption mechanism in RPLC [29–37]. The migration velocity, $u(C)$ of the acetonitrile wave of concentration C along the column is given by [30,31]:

$$u(C) = \frac{u_0}{1 + (S/V_M)(d\Gamma/dC)} \quad (14)$$

where S is the surface area available in the column, V_M is the thermodynamic void volume, Γ is the unique excess adsorbed amount of acetonitrile, and C is the concentration of acetonitrile in the bulk. On endcapped silica-C_{18} stationary phases, the derivative in the right hand side of this equation is negative and close to its steepest value for $\varphi = 0.70$ [32]. This holds true for a large range of surface coverages, from 0 (only C_1 endcapped) to 3.2 μmol/m^2 [34]. Accordingly, the wave concentrations of acetonitrile migrate faster than u_0 and the gradient cannot be considered to be linear (due to a non-linear distortion [38]) nor to move at a constant speed u_0.

Fig. 1 proves this effect right at the optimum flow rate of 1.5 mL/min. The chromatogram shows that the initial baseline perturbation (the slightly parabolic drift) caused by the change in the mixing volume ratio of the pumps is detected approximately at $t = 0.80$ min, a time that is shorter than what was expected, the sum of the dwell time and the hold-up time (*i.e.* $t_D + t_0 = 0.08 + 0.87 = 0.95$ min) if the gradient was propagating at the constant velocity u_0.

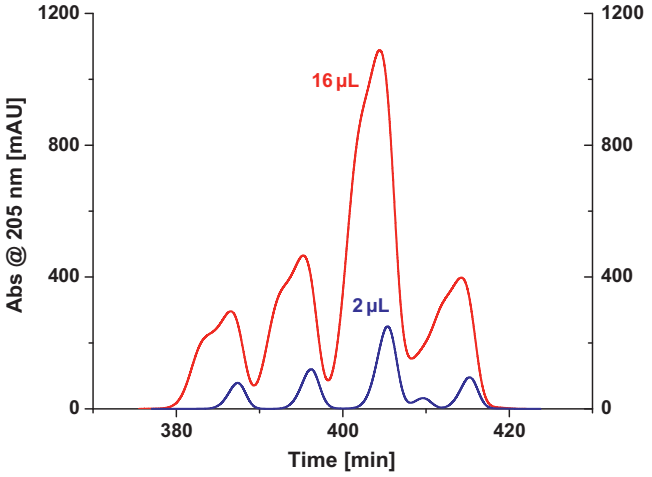

Fig. 8. Negative effect of too large an injected volume of the sample solution on the peak capacity. Same experimental conditions as in Fig. 1, except the flow rate F_v = 1 mL/min.

4.3.2. Optimum injection volume

The injection volume was increased from 0.2, to 0.5, 1.0, 2.0, 4.0, 8.0, 12.0 and to 16.0 µL. The flow rate was kept at 1 mL/min, fixing the gradient time at 6.5 min. Fig. 8 compares the chromatograms recorded after injecting 2 and 16 µL sample volumes. A zoom was made around the five last eluted compounds. This figure provides a striking illustration of how too large an injected volume can significantly deteriorate the quality of a gradient separation. A shoulder appears and progressively grows on the front part of each peak when the injected volume is increased and becomes larger than 2 µL. The peak capacity drops from 63 (when V_{Inj} = 2 µL), to 57 (4 µL), 53 (8 µL), 34 (12 µL) to 29 (16 µL). Therefore, the injected volume was kept at 2 µL.

4.3.3. Optimum column length

If at a fixed temperature (here T = 295 K), the gradient parameters S (here 10.1), $\Delta\varphi$ (here 0.27), and t_G/t_0 (here 4.95), are kept constant, the last experimental parameter that could be adjusted is the column length. According to Eqs. (2) and (6), increasing the square root of the column length should lead to a linear increase of the peak capacity. Therefore, the column length was increased from 15, to 25, 35 and to 45 cm by successively coupling up to three additional 4.6 mm × 100 mm Kinetex-C_{18} columns. The optimal flow rate was kept at 1.5 mL/min, as justified previously. The maximum inlet pressures recorded before the gradient starts (70% acetonitrile) were 366, 573, 745, and 930 bar, respectively.

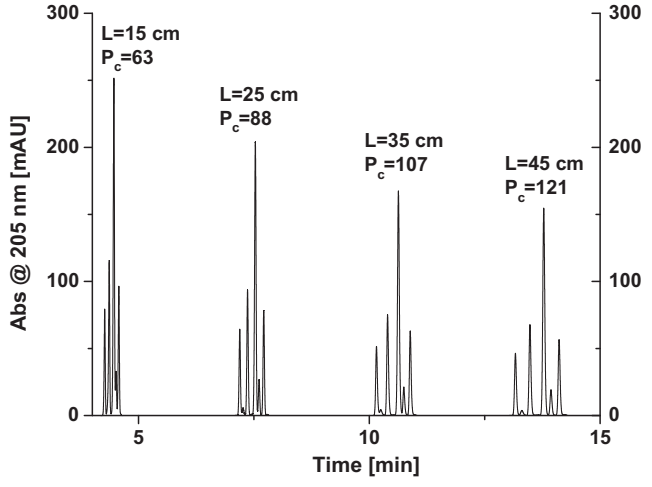

Fig. 9. Effect of the column length on the separation of the last eluted fraction of compounds produced by *B. braunii*. Same experimental conditions as those in Fig. 1.

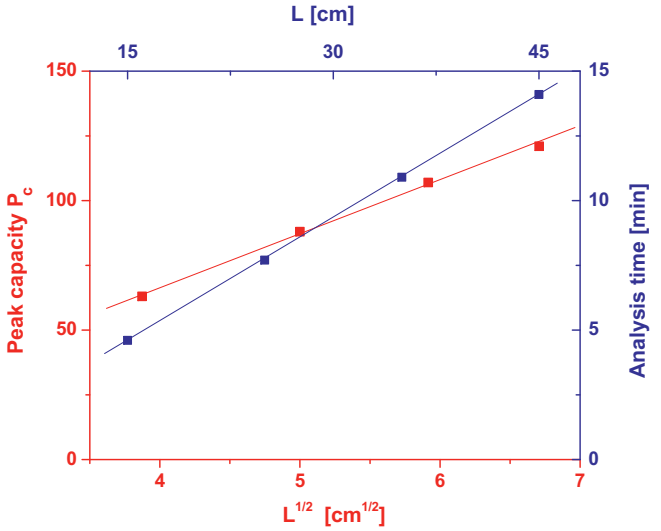

Fig. 10. Plots of the peak capacity and the analysis time versus the column length. Temperature T = 297 K. LSSM parameter S = 10.1. Amplitude of the gradient $\Delta\varphi$ = 0.27. Ratio of the gradient time to the hold-up time t_G/t_0 = 4.95. Same experimental conditions as those in Fig. 1.

Fig. 9 illustrates how the resolution of the most abundant compounds improves with increasing the column length from 15 to 45 cm. The peak capacity of 63 for a 15 cm long column increases to 88, 107, and 121 for column lengths of 25, 35, and 45 cm, respectively, in excellent agreement with the theoretical predictions ($P_c \propto \sqrt{L}$) as shown in Fig. 10. Obviously, the gain in peak capacity has to be paid by a parallel increase of the analysis time while the sensitivity of the method remains nearly constant.

5. Conclusion

The hydrocarbons extracted from cultures of the green microalgae *B. braunii* exposed to nutrition stress were analyzed by gradient HPLC, using columns packed with core–shell particle columns. The range of elution times of the eluted compounds compared to that of squalene ($C_{30}H_{50}$), suggests that no measurable amount of C_{30} or heavier (methylated derivatives) botryococcenes could be detected after a period of seven days of nutritional stress. In contrast, large amounts of hydrocarbons with lower molecular weights were easily detected by UV detection. The quality of the final separation of these biofuel precursors using acetonitrile/water gradient elution on a set of four 4.6 mm I.D. Kinetex-C_{18} columns was acceptable. Optimum gradient elution conditions were found by keeping the initial and final acetonitrile concentrations at 70% and 97%, respectively. The flow rate was adjusted to minimize the column plate height under isocratic conditions. It was found critical to keep the injection volume smaller than 2 µL to prevent serious losses in peak capacity caused by volume and possibly concentration overloading. Finally, the largest column length that could be used was 45 cm (providing a total pressure drop of 930 bar) before the beginning of the gradient. The combination of these experimental conditions gave a maximum peak capacity of 121, with a retention window of 11.4 min, which provided a complete resolution of the most abundant compounds detected in the extracted mixture. Obviously, operating columns at higher temperatures would have allowed the use of a larger number of them, columns, *e.g.* to achieve a significant increase of the peak capacity for the same analysis time. From a practical point of view, this first gradient HPLC analysis of the

chloroform extract of *B. braunii* shows that the experimental conditions required for the production, extraction, and concentration of botryococcennes have not yet been fully optimized. In a forthcoming report, the results of similar analyses made on colonies of *B. braunii* exposed to a series of light irradiation with a range of wavelengths from red to UV and intensities will be presented. The extraction/re-concentration protocols of the hydrocarbons will be improved. The production of low molecular weight hydrocarbons and of botryococcenes will be analyzed by HPLC. Additionally, HPLC analysis will be coupled with mass spectrometry in order to measure the masses of the hydrocarbon molecules produced by the green algae. Soft assisted proton ionization will be applied to ionize the sample molecules without breaking any C–C or C=C bonds. From a more fundamental point of view, the trends of the measured peak capacities with increasing flow rates and column lengths were found to be in excellent agreement with the theoretical predictions, provided that it is recognized that the propagation velocity of the gradient along the column (the propagation of the concentration waves) is much faster than the chromatographic linear velocity, u_0. This possibly explains why the absolute value of the experimental peak capacities were slightly smaller than the theoretical ones (−9% when assuming no band compression and −20% when assuming peak compression during gradient elution). In fact, the gradient of mobile phase concentration was run over a range of acetonitrile concentration ($0.70 < \varphi < 0.97$) within which excess adsorption onto an endcapped silica-C_{18} adsorbent decreases rapidly with increasing acetonitrile concentration. This observation deserves more careful attention when estimating the organic content at the column outlet, at the time when the last few compounds are eluting. Current gradient theories should be adjusted in order to account quantitatively for the impact of distorted gradient elution profile (caused by steep variations of the excess adsorption of the strong solvent) on the peak capacities.

List of symbols

Roman letters

F_v	flow rate (m^3/s)
G	intrinsic gradient steepness ($= S\Delta\varphi(t_0/t_G)$)
H	total column HETP (m)
$\overline{H}$	average total column HETP experienced by the sample during gradient elution (m)
k	retention factor
k_0	retention factor in pure water
k_F	apparent retention factor of the last eluted compound in gradient conditions
k_{last}	retention factor of the last eluted compound at the beginning of the gradient
L	column length (m)
P_c	peak capacity
t	time variable (s)
t_0	column hold-up time (s)
t_{last}	elution time of the last eluted compound in gradient conditions (s)
t_G	gradient time (s)
t_I	elution time of the first eluted compound in gradient conditions (s)
S	negative of the slope of the LSSM plot
S_{last}	LSSM slope parameter of the last eluted compound in gradient conditions
T	temperature during the HETP experiments (K)

Greek letters

φ	volume fraction of acetonitrile in the mobile phase
φ_{start}	volume fraction of acetonitrile at the beginning of the gradient
φ_{end}	volume fraction of acetonitrile at the end of the gradient
$\varphi_{z=0}$	volume fraction of acetonitrile at the column inlet
$\varphi_{z=L}$	volume fraction of acetonitrile at the column outlet
$\Delta\varphi$	amplitude of the change in volume fraction during the gradient
ψ	parameter defined in Eq. (8)
σ	peak standard deviation (s)
ω	parameter defined in Eq. (7)
ω_i	baseline peak width of compound i (s)

Acknowledgments

This work was supported in part by the cooperative agreement between the University of Tennessee and the Oak Ridge National Laboratory.

References

[1] Q. Hu, M. Sommerfeld, E. Jarvis, M. Ghirardi, M. Posewitz, M. Seibert, A. Darzins, Plant J. 54 (2008) 621.
[2] Y. Chisti, Trends Biotechnol. 26 (2008) 126.
[3] Y. Chisti, Biotechnol. Adv. 25 (2007) 294.
[4] Chemicals from Microalgae, Taylor and Francis, 1999.
[5] P. Metzger, E. Casadevall, M. Pouet, Y. Pouet, Phytochemistry 24 (1985) 2995.
[6] T. Weiss, H. Chun, S. Okada, S. Vitha, A. Holzenburg, J. Laane, T. Devarenne, J. Biol. Chem. 285 (2010) 32458.
[7] P. de Mesmay, P. Metzger, V. Grossi, S. Derene, Phytochemistry 39 (2008) 879.
[8] F. Gritti, G. Guiochon, J. Chromatogr. A (2011), doi:10.1016/j.chroma.2011.07.014.
[9] F. Gritti, G. Guiochon, J. Chromatogr. A 1221 (2011) 2.
[10] G. Guiochon, N. Marchetti, K. Mriziq, A. Shalliker, J. Chromatogr. A 1189 (2008) 109.
[11] J.J. DeStefano, T.J. Langlois, J.J. Kirkland, J. Chromatogr. Sci. 46 (2007) 254.
[12] F. Gritti, A. Cavazzini, N. Marchetti, G. Guiochon, J. Chromatogr. A 1157 (2007) 289.
[13] F. Gritti, I. Leonardis, D. Shock, P. Stevenson, A. Shalliker, G. Guiochon, J. Chromatogr. A 1217 (2010) 1589.
[14] F. Gritti, G. Guiochon, J. Chromatogr. A 1217 (2010) 3819.
[15] F. Gritti, G. Guiochon, J. Chromatogr. A 1217 (2010) 1604.
[16] U. Neue, J. Chromatogr. A 1079 (2005) 153.
[17] H. Poppe, J. Paanakker, J. Bronckhorst, J. Chromatogr. 204 (1981) 77.
[18] F. Gritti, G. Guiochon, J. Chromatogr. A 1145 (2007) 67.
[19] F. Gritti, G. Guiochon, J. Chromatogr. A 1178 (2008) 79.
[20] F. Gritti, G. Guiochon, J. Chromatogr. A 1212 (2008) 35.
[21] F. Gritti, G. Guiochon, J. Chromatogr. A 1215 (2008) 64.
[22] F. Gritti, G. Guiochon, J. Chromatogr. A 1216 (2009) 6124.
[23] P. Jandera, J. Churacek, Gradient Elution in Column Liquid Chromatography—Theory and Practice, Elsevier, Amsterdam, 1985.
[24] L. Snyder, J.J. Kirkland, J.W. Dolan, Introduction to Modern Liquid Chromatography, 3rd ed., Wiley-Interscience, New York, 2010.
[25] F. Gritti, G. Guiochon, J. Chromatogr. A, in preparation.
[26] F. Gritti, G. Guiochon, Chem. Eng. Sci. 65 (2010) 6327.
[27] M. Gao, B. Simoneit, M. Gantar, S. Jaffè, Chemosphere 70 (2007) 224.
[28] A. Krstulovic, H. Colin, A. Tchapla, G. Guiochon, Chromatographia 17 (1983) 228.
[29] R.M. McCormick, B. Karger, Anal. Chem. 52 (1980) 2249.
[30] Y. Kazakevich, H. McNair, J. Chromatogr. Sci. 31 (1993) 317.
[31] Y. Kazakevich, H. McNair, J. Chromatogr. Sci. 33 (1995) 321.
[32] F. Gritti, G. Guiochon, Anal. Chem. 77 (2005) 4257.
[33] F. Gritti, G. Guiochon, J. Chromatogr. A 1155 (2007) 85.
[34] F. Gritti, G. Guiochon, J. Chromatogr. A 1169 (2007) 111.
[35] S. Bocian, A. Felinger, B. Buszewski, Chromatographia 68 (2008) S19.
[36] S. Bocian, P. Vajda, A. Felinger, B. Buszewski, J. Chromatogr. A 1204 (2008) 35.
[37] B. Buszewski, S. Bocian, G. Rychlicki, P. Vajda, A. Felinger, J. Colloid Interface Sci. 349 (2010) 620.
[38] T. Ahmad, F. Gritti, B. Lin, G. Guiochon, Anal. Chem. 76 (2004) 977.